Sucrose synthase determines carbon allocation in developing wood and alters carbon flow at the whole tree level in aspen

Pia Guadalupe Dominguez[1] (iD), Evgeniy Donev[1]* (iD), Marta Derba-Maceluch[1]* (iD), Anne Bünder[1], Mattias Hedenström[2] (iD), Ivana Tomášková[3] (iD), Ewa J. Mellerowicz[1] (iD) and Totte Niittylä[1] (iD)

[1]Umeå Plant Science Centre, Department of Forest Genetics and Plant Physiology, Swedish University of Agricultural Sciences, Umeå 90183, Sweden; [2]Department of Chemistry, Umeå University, Umeå 90187, Sweden; [3]Department of Genetics and Physiology of Forest Trees, Faculty of Forestry and Wood Sciences, Czech University of Life Sciences Prague, Prague 165 00, Czech Republic

Summary

- Despite the ecological and industrial importance of biomass accumulation in wood, the control of carbon (C) allocation to this tissue and to other tree tissues remain poorly understood.
- We studied sucrose synthase (SUS) to clarify its role in biomass formation and C metabolism at the whole tree level in hybrid aspen (*Populus tremula* × *tremuloides*). To this end, we analysed source leaves, phloem, developing wood, and roots of *SUSRNAi* trees using a combination of metabolite profiling, $^{13}CO_2$ pulse labelling experiments, and long-term field experiments.
- The glasshouse grown *SUSRNAi* trees exhibited a mild stem phenotype together with a reduction in wood total C. The $^{13}CO_2$ pulse labelling experiments showed an alteration in the C flow in all the analysed tissues, indicating that SUS affects C metabolism at the whole tree level. This was confirmed when the *SUSRNAi* trees were grown in the field over a 5-yr period; their stem height, diameter and biomass were substantially reduced.
- These results establish that SUS influences C allocation to developing wood, and that it affects C metabolism at the whole tree level.

Introduction

Wood biomass is a valuable raw material for wood-based industries including pulp, paper, sawn timber, and biofuel production (Plomion *et al.*, 2001; Novaes *et al.*, 2009). Wood formation depends on carbon (C) allocation to developing wood. In several tree species, C is distributed predominantly as sucrose (Rennie & Turgeon, 2009). Phloem loading in source leaves of the model tree aspen (*Populus tremula* L.) occurs via a symplasmic route (Zhang *et al.*, 2014). Phloem unloading mechanism into developing wood is less well understood but is thought to include both symplasmic and apoplasmic steps (Van Bel, 1990; Chaffey & Barlow, 2001; Mahboubi *et al.*, 2013). Despite our increasing understanding of C transport routes in trees, the mechanism of C allocation and biomass accumulation in the different tissues remain poorly understood.

Biomass formation depends partly on the capacity of the wood tissue and other C competitor sink tissues such as shoot and root meristems to metabolize and incorporate C (Yu *et al.*, 2015). Primary metabolic reactions are especially important in this process because they are responsible for sucrose catabolism, energy production, and the synthesis of the precursors for cell wall polymers. Studies on biomass accumulation in trees commonly focus

on hormonal factors and C allocation to cell wall polymers (Dubouzet *et al.*, 2013; Busov, 2018), while primary metabolism has received less attention (Mahboubi & Niittylä, 2018). The C availability for biomass production by sink tissues depends on the photosynthetic and sucrose export capacity of source leaves (Yu *et al.*, 2015); in recognition of this, efforts have been made to increase wood biomass by improving tree photosynthesis (Dubouzet *et al.*, 2013; Busov, 2018). However, C acquisition, allocation, and metabolism in the different tissues of a tree depend on the relationship between sink and source tissues, which should therefore be considered jointly (Sonnewald & Fernie, 2018).

The concept of sink strength refers to a sink tissue capacity to compete for photoassimilates. This is determined by the capacity of the tissue to import C from the leaves and to synthesize macromolecules (Yu *et al.*, 2015). The capacity for C import depends in part on enzymes that degrade sucrose. Two types of enzymes catalyse sucrose degradation in sink tissues: sucrose synthase (SUS) and invertase. SUS has been associated with C allocation, increased biomass, and sink strength (Stein & Granot, 2019). It is known to be the main sink strength determinant in potato tubers (Zrenner *et al.*, 1995), and to control C import in young tomato fruits (D'Aoust *et al.*, 1999). In tobacco plants, SUS overexpression increased height and biomass, indicating that it can also control C allocation in this species (Coleman *et al.*, 2006).

*These authors contributed equally to this work.

Conversely, evidence from rice and corn suggests that acid invertases are the main grain sink strength determinants in these species (Cheng *et al.*, 1996; Li *et al.*, 2013; Morey *et al.*, 2018). The relative impacts of SUS and invertase on C allocation thus appear to depend on the tissue, species, developmental stage, and season. Consequently, it is impossible to predict the contributions of these two enzymes to C metabolism a priori.

We previously observed decreased wood density in aspen trees with reduced SUS levels, which was accompanied by a decrease in cellulose, hemicellulose, and lignin content per unit volume of wood (Gerber *et al.*, 2014). The decrease in total polymer biomass per unit volume suggested reduced C incorporation into wood cell walls. Moreover, expression of a cotton SUS in aspen trees increased cell wall thickness and wood density (Coleman *et al.*, 2009), while aspen SUS expression in tobacco plants increased xylem cell wall thickness (Wei *et al.*, 2015). These observations support a central role for SUS in C allocation to wood, but they do not reveal the role of SUS in C allocation and metabolism, and biomass accumulation at the whole tree level. This prompted us to study the role of SUS at the whole tree level under glasshouse and field conditions using transgenic *SUSRNAi* lines. The assessment of the C metabolism was performed by combining total metabolite pool measurements and the tracking of a carbon-13 (^{13}C) flow among the central metabolites in leaves, phloem, developing wood and roots after $^{13}CO_2$ supply.

Materials and Methods

Plant material

Three *35S:SUSRNAi* transgenic lines (Gerber *et al.*, 2014) along with wild-type (WT) T89 hybrid aspens (*Populus tremula × tremuloides*) were grown in a glasshouse in commercial soil (Yrkes Plantjord; SW Horto, Hammenhög, Sweden) under an 18 h : 6 h, 20°C : 15°C, light : dark photoperiod. Trees were fertilized using 150 ml 1% Rika-S (nitrogen (N)–phosphorus (P)–potassium (K), 7 : 1 : 5; SW Horto) once a week, and were harvested when they were 2 months old. Wood samples were collected from 15 to 45 cm above the soil. In the field experiment, the same genotypes were grown for 5 yr in a field setting in Våxtorp, Laholm community, Sweden (56.42°N, 13.07°E). Trees were planted with a 3 m spacing in 2011. Four trees per each transgenic line and 32 WT trees were randomly distributed over the field area. The field was harrowed twice a year during the first 2 yr following planting and grass was mowed twice a year during subsequent years. Height and diameter (at the stem base) were measured at the end of each growing season and before harvest in the summer 2016.

Sample preparation

All samples were frozen on liquid nitrogen immediately after collection and stored at −80°C until preparation. Developing wood from both glasshouse and field trees was obtained by scrapping the surface of frozen debarked stems with a scalpel while maintaining the low temperature with liquid nitrogen. Phloem samples were obtained by scrapping the inner side of the barks. Fully expanded leaves number 14–16 (counting from the top) were sampled. The tips of the roots were cut, cleaned and immediately frozen. All the obtained frozen tissues were ground with a mortar and pestle. The ground material was kept at −80°C until use.

Sucrose synthase activity determination in glasshouse grown trees

The protocol was based on that of Gerber *et al.* (2014). Extracted samples (extraction buffer: 100 mM Tris-HCl pH 7.5, 2 mM EDTA, 5 mM DTT, a scoop of PVPP; Roche proteinase inhibitor, Roche, Basel, Switzerland) were incubated with 45 μl of reaction mix (100 mM Tris pH 7.5, 100 mM sucrose, 4 mM UDP (uridine diphosphate)) for 30 min at 25°C. A control for each sample was prepared simultaneously using 45 μl of reaction mix without UDP. The reaction product, UDP–glucose, was determined by incubating 25 μl (developing wood) or 100 μl (roots) of the reaction mix with 25 μl of the determination buffer (100 mM Tris pH 7.5, 2 mM NAD$^+$, 0.02 u UGDH) at 340 nm. The absorbances were interpolated into a UDP–glucose standard curve. Total protein contents were determined by using the DC Protein Assay (Bio-Rad, Hercules, CA, USA).

Quantitative polymerase chain reaction (qPCR) in glasshouse and field grown trees

Total mRNA was extracted with Trizol® (Gibco, Gaithersburg, MD, USA) according to the manufacturer´s specifications. The cDNA was prepared using the MessageAmp Premier RNA Amplification Kit (Ambion, Austin, TX, USA). The reference gene was *Ubiquitin*, which was chosen based on its transcript stability. Quantitative polymerase chain reactions (qPCRs) were performed using SYBR® Green Master Mix (Bio-Rad) in a CFX96 Real Time System (Bio-Rad) with the following programme: 95°C for 5 min, then 50 cycles of 95°C for 30 s, 60°C for 15 s, and 72°C for 30 s. The employed primers are listed in Supporting Information Table S1. Primers were designed with PRIMER3 (Untergasser *et al.*, 2012). Ratios were calculated using the equation proposed by Pfaffl (2001): $\text{Ratio} = (E_{\text{target}})^{\Delta Cp \ \text{target(MEAN control − MEAN sample)}} ((E_{\text{reference}})^{\Delta Cp \ \text{reference(MEAN control − MEAN sample)}})^{-1}$.

Dry weight and total C phenotype

Tissues from 2-month-old or 5-yr-old trees were dried for 1 wk at 80°C to measure the dry weight. Total C from tissues of glasshouse-grown trees was measured by elemental analyser-isotope ratio mass spectrometry (EA-IRMS; Thermo Fisher Scientific, Waltham, MA, USA). Furthermore, 5 mg of oven-dried sample were employed for each measurement. Measurements were performed with an elemental analyser (Flash EA 2000; Thermo Fisher Scientific) connected to a continuous flow isotope ratio mass spectrometer (DeltaV) (Thermo Fisher Scientific). Samples were analysed together with cyclohexanone, nicotinamide, and sucrose standards, which were standardized against standard reference materials. Data were corrected for drift and size.

Photosynthetic parameters in glasshouse grown trees

The leaf nitrogen balance index (NBI), chlorophyll index (CHL), flavonol index (FLV), and anthocyanin index (ANTH) were measured with a Force A Dualex Scientific+™ device on 10 independent plants at midday. Chlorophyll a fluorescence (ChlF) measurements were performed on 10 leaves per plant over five consecutive days from 09:00 h to 16:00 h using a FluorPen FP100max portable fluorometer (Photon Systems Instruments, Brno, Czech Republic). The kinetics of chlorophyll fluorescence induction were estimated based on the polyphasic rise of the ChlF transient (OJIP) curve using the calculations proposed by Stirbet & Govindjee (2011). The second employed protocol applied with the FluoPen fluorometer was the Light Curve protocol (protocol LC3) using the calculations proposed by Maxwell & Johnson (2000).

^{13}C labelling experiment in glasshouse grown trees

A Percival Scientific cabinet with a CO_2 system (model: PGC-7L2) was employed to supply $^{13}CO_2$ (> 99 atom%, > 99.98%; BOC UK & Ireland, Bluebell, Dublin, Ireland) to the trees. When the experiment started, $^{12}CO_2$ was removed from the air in the chamber using the chamber's in-built CO_2 scrubbing system, and $^{13}CO_2$ was quickly injected up to 400 ppm. The $^{13}CO_2$ was re-injected whenever its levels fell below 350 ppm. The CO_2 levels were measured with a WMA-4 CO_2 analyser (www.ppsystems.com). Groups of four plants were injected with $^{13}CO_2$ on each experimental run, and were sampled after 4, 6 and 8 h of treatment. Unlabelled controls for each genotype were injected with $^{12}CO_2$ in the same chamber, and sampled at 6, 8, 10 and 14 h after the start of the light period, covering the times of the day in which ^{13}C labelling was performed on the experimental plants. The generated labelled material was analysed by gas chromatography mass spectrometry (GC-MS) and/or two-dimensional nuclear magnetic resonance (2D-NMR) as described later. Only metabolites with slow labelling rates (data obtained from Szecowka et al., 2013) were examined to minimize the influence of potential ^{12}C incorporation during sampling.

GC-MS measurements

All the labelled samples and controls were analysed by GC-MS. Frozen samples (10 mg) were extracted with 1 ml of a chloroform–methanol–water (20 : 60 : 20, v/v/v) solution containing two stable isotope reference compounds (7 ng µl^{-1} [$^{13}C_3$]-myristic acid and [$^2H_7$]-cholesterol). N-Methyl-N-(trimethylsilyl)trifluoroacetamide (MSTFA) was used as a reagent for silylation derivatization done according to Lindén et al. (2016). The GC-MS protocol was based on that of Gullberg et al. (2004). Thus, 1 µl of each derivatized sample was injected in splitless mode per run. The GC-MS system used electron impact (EI) ionization and consisted of a CTC PAL systems autosampler (CTC Analytics AG, Zwingen, Switzerland), an Agilent technologies 7890A GC system (Agilent Technologies, Atlanta, GA, USA), and a Pegasus HT GC high-throughput TOF-MS instrument (LECO

Corp., St Joseph, MI, USA). The analysed fragments for the labelling calculations were selected based on Lindén et al. (2016) and Beshir et al. (2017). Corrections for the ^{13}C natural abundance and the presence of tetramethylsilane (TMS) groups, and computations of ^{13}C enrichment percentages for each identified metabolite were performed as described by Mahboubi et al. (2015) and Lindén et al. (2016).

2D-NMR analysis

The protocol was based on that of Hedenström et al., 2009. Developing wood samples belonging to SUSRNAi-1 and WT with no label (time 0) and labelled for 8 h (time 8) were analysed by 2D-NMR. Before analyses, soluble sugars and starch were removed from the samples as described in Smith & Zeeman (2006) to avoid signal interferences in the cell wall NMR measurements. Next, 20 mg of ground tissues were added to 600 µl of deuterated dimethyl sulfoxide (DMSO-d_6). The 2D ^1H-^{13}C heteronuclear single quantum coherence (HSQC) experiments were performed on a Bruker 600 MHz Avance III HD spectrometer equipped with a 5 mm BBO cryoprobe with z-gradients (Bruker Biospin, Rheinstetten, Germany). All measurements were performed at 25°C. In the pulse sequence, adiabatic ^{13}C-inversion and ^{13}C-refocusing pulses were used (Bruker pulse sequence hsqcetgpsisp.2). The sweep width was 10 ppm for the ^1H dimension and 165 ppm for the ^{13}C dimension. Processing and peak integration were performed using Topspin 3.6 (Bruker Biospin). The peak assignments were based on that of Kim et al. (2008).

Starch content measurement in glasshouse grown trees

Briefly, 10 mg of the tissues were extracted with 250 µl of 80% v/v ethanol and gelatinized according to Smith & Zeeman (2006). Next, 40 µl of the resuspension was treated with 6 U of alpha-amyloglucosidase and 0.5 U of alpha-amylase prepared in 50 mM acetate buffer. Negative controls were processed in the same way using 50 mM acetate buffer without the enzymes. The tubes were incubated at 37°C overnight. The treatment with the enzymes was done twice for phloem, developing wood and mature wood, and three times in the leaf samples to assure a complete starch degradation. Then, 50 µl of the samples or controls were then incubated with 75 µl of the determination buffer (HEPES pH 7.5 50 mM, NADP 0.4 mM, ATP 2 mM, G6P DHG 2 U ml^{-1}, HXK 2 U ml^{-1}, PGI 2 U ml^{-1}). The absorbances were interpolated into a glucose standard curve.

Acid invertase activity determination in glasshouse grown trees

The protocol was based on that of Hubbard et al. (1989). Developing wood samples (10 µl each) were incubated with 45 µl of reaction buffer (25 mM citrate phosphate buffer, pH 5, and 25 mM sucrose) for 1 h at 25°C. A control for each sample was prepared in parallel replacing the reaction buffer with 25 mM citrate phosphate buffer pH 5. Then, 50 µl of the reaction mix

was then incubated with 75 µl of the determination buffer (HEPES pH 7.5 50 mM, NADP 0.4 mM, ATP 2 mM, G6P DHG 2 U ml^{-1}, HXK 2 U ml^{-1}, PGI 2 U ml^{-1}). The absorbances measured at 340 nm were interpolated into a glucose standard curve.

Neutral invertase activity determination in glasshouse grown trees

The protocol was based on that of Rende et al. (2016). Briefly, 1 µl of each sample extract (extraction buffer: 50 mM HEPES pH 7, 10 mM MgCl$_2$, 1 mM EDTA, 0.25 mM DTT, 1% Triton X-100, 20% glycerol; Roche proteinase inhibitor) was incubated with 75 µl of the determination buffer (50 mM HEPES pH 7, 0.4 mM NADP$^+$, 2 mM ATP, 2 U ml^{-1} glucose-6-phosphate dehydrogenase, 2 U ml^{-1} hexokinase, 2 U ml^{-1} phosphoglucose isomerase). Then, 20 µl of 100 mM sucrose was added to each mixture to initiate the reactions. Controls for each sample were prepared in parallel replacing the 100 mM sucrose with HEPES pH 7. Absorbances measured at 340 nm were interpolated into a glucose standard curve.

Statistical analyses

All experiments were analysed statistically by analysis of variance (ANOVA), using Duncan's multiple range test (MRT) for multiple comparison. All analyses were performed with the INFOSTAT software (v.2008; Infostat Universidad Nacional de Córdoba, Argentina). A significance threshold of $P < 0.05$ was applied. The three-dimensional (3D) principal component analysis (PCA) scatter plot was created with BIOVINCI software (BioTuring Inc., San Diego, CA, USA).

Results

SUSRNAi reduces SUS activity in developing wood and roots

The Populus genome contains seven SUS genes, named SUS1–SUS7 (Zhang et al., 2011). The SUSRNAi construct targets SUS1 and SUS2, which are the most strongly expressed isoforms in developing wood (Zhang et al., 2011; Gerber et al., 2014). SUS1 and SUS2 transcripts are also found in leaves and roots (Zhang et al., 2011), suggesting that the RNAi construct may also reduce the total SUS activity in these tissues. To clarify the SUSRNAi effects at the whole tree level, we measured SUS activity in developing wood, roots, and source leaves. In accordance with our previous results, SUS activity was reduced to near background levels in developing wood of the SUSRNAi lines (Fig. 1a), while in roots its activity was reduced to 40% of the WT level (Fig. 1b). The more modest reduction in roots is probably partly due to the expression of other SUS isoforms (Zhang et al., 2011). The SUS activity in the source leaf extracts of WT trees was close to background levels. Therefore, to assess the SUSRNAi effects in source leaves, we quantified the mRNA levels of all the SUS isoforms using qPCR. Only SUS1 and SUS5 transcript levels in the

three transgenic lines were reduced to c. 30% and 50%, respectively, of the WT levels (Fig. 1c). The reduction in SUS5 mRNA levels is not a direct SUSRNAi effect, because the percentage of similarity between the nucleotide coding regions of SUS1 and SUS5 is c. 58% (Zhang et al., 2011) and the SUSRNAi does not target SUS5.
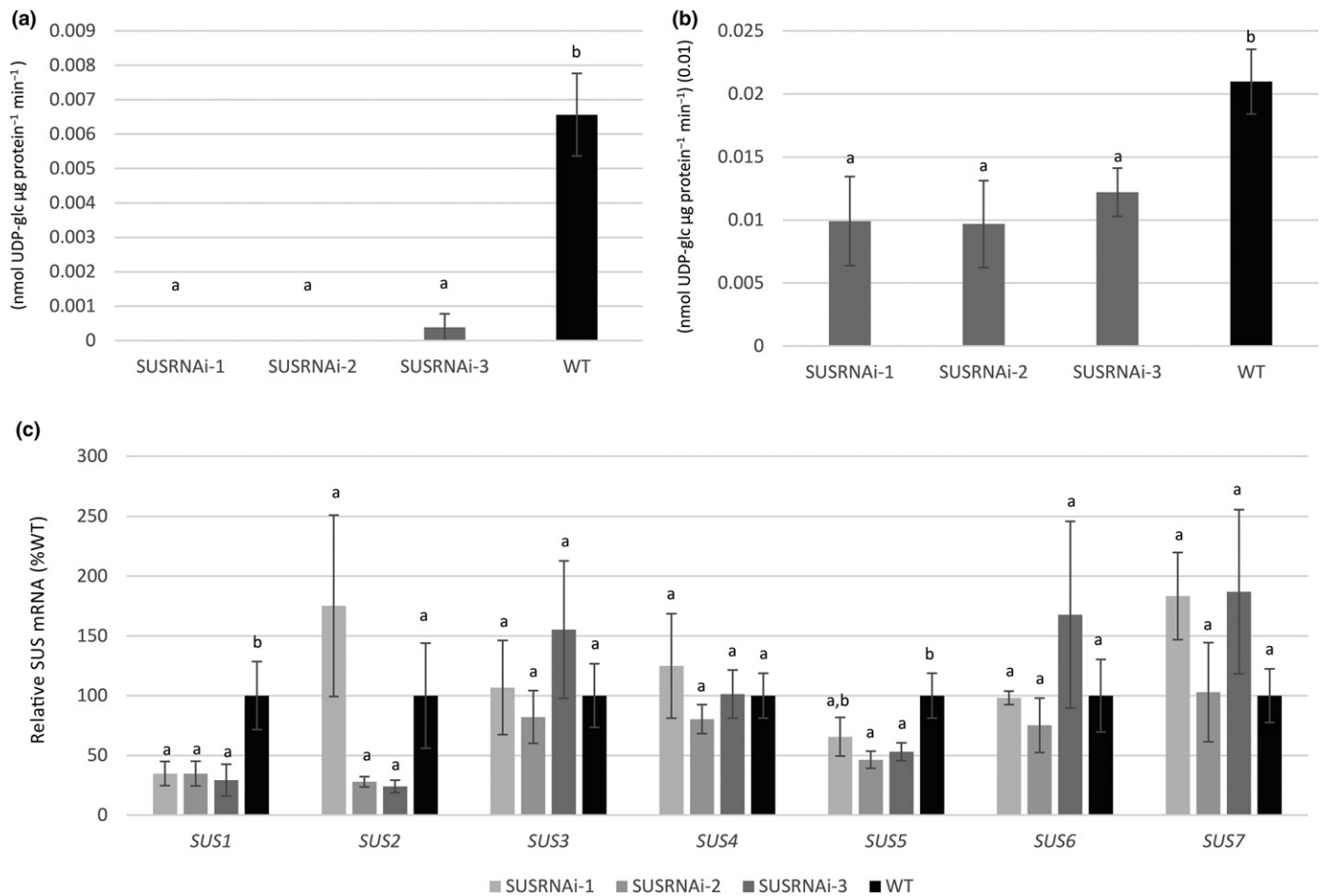
Total C is reduced in developing wood of SUSRNAi lines

We performed detailed growth phenotyping of 2-month-old glasshouse grown SUSRNAi trees. The total stem fresh weight of the glasshouse-grown transgenic lines did not differ significantly from that of the WT (Fig. 2a). However, the stem dry weight of the transgenics was slightly reduced, being statistically significant in SUSRNAi-3 (Fig. 2b). Moreover, the total C content in developing wood as measured by IRMS was significantly reduced in all the silenced lines (Fig. 2c), clearly indicating that the C allocation to this tissue was reduced. These observations are consistent with our previous results documenting reduced stem wood density and increased fibre wall shrinkage upon drying in the SUSRNAi lines (Gerber et al., 2014). The total leaf fresh and dry weight were unchanged in the transgenic lines, except in SUSRNAi-3 (Fig. 2d,e). The total root fresh and dry weight were unchanged in all lines (Fig. 2g,h), as was the total C content in leaves and roots (Fig. 2f,i). Therefore, the growth defect in the SUSRNAi lines is primarily associated with wood formation, and not with leaf and root growth.

Photosynthetic light-dependent reactions are not affected in the SUSRNAi source leaves

Alterations in sugar metabolism can cause alterations in photosynthesis (Sheen, 1990). To determine whether the photosynthetic performance of the source leaves in transgenic genotypes contributed to the reduction in the developing wood C content, we assayed leaf pigments and the photosynthesis light-dependent reactions. CHL, ANTH, FLV, and NBI (i.e. the ratio of the chlorophyll and flavonol indexes) showed no significant differences (Table S2). The photosynthesis light-dependent reactions can be evaluated by measuring the ChlF and computing different parameters like those of OJIP and LC (light curve) that provide information on the condition of the photosystem II and the electron transport in the thylakoid membrane. OJIP shows how the photochemical efficiency varies under different light conditions (Baker, 2008). The OJIP test equations were therefore used to calculate parameters including the PI$_{abs}$, the F_v/F_m ratio, and the specific fluxes for the reaction centres (Table S3). All the tested genotypes had PI$_{abs}$ values of c. 4 and F_v/F_m values between 0.80 and 0.83, indicating that the primary photochemical reactions do not show changes. The specific energy fluxes values involving the reaction centres (ABS/RC and ETo/RC) were higher in the SUSRNAi-1 line than in WT trees. However, the values of the other photosynthetic parameters in the SUSRNAi-1 line and all the photosynthetic parameters in the other SUSRNAi lines were comparable to those in WT trees. The computed LC parameters, which relate the photosynthesis rate to the photon flux density,

Fig. 1 SUS activity in 2-month-old wild-type (WT) and *SUSRNAi* hybrid aspen (*Populus tremula* × *tremuloides*) trees grown in the glasshouse and measured in (a) developing wood, and (b) in roots, (c) *SUS* mRNA abundance in source leaves measured by RT-qPCR. ANOVA, Duncan test, $n = 5$–4. Different letters indicate significant differences ($P < 0.05$). Bars indicate the average and error bars indicate the standard error.

included F_t, Q_y, F_0 and F_m (Table S4). No consistent differences were observed between WT and *SUSRNAi* lines, indicating that the photosynthesis is not affected by the light intensity in the transgenics. Based on these results, it can be concluded that *SUSRNAi* does not affect pigment levels or the photosynthetic performance in source leaves. Its effects on wood are thus not due to impaired photosynthesis light-dependent reactions but more likely due to changes at the leaf metabolic level, leaf-to-wood C transport, and/or developing wood metabolism.
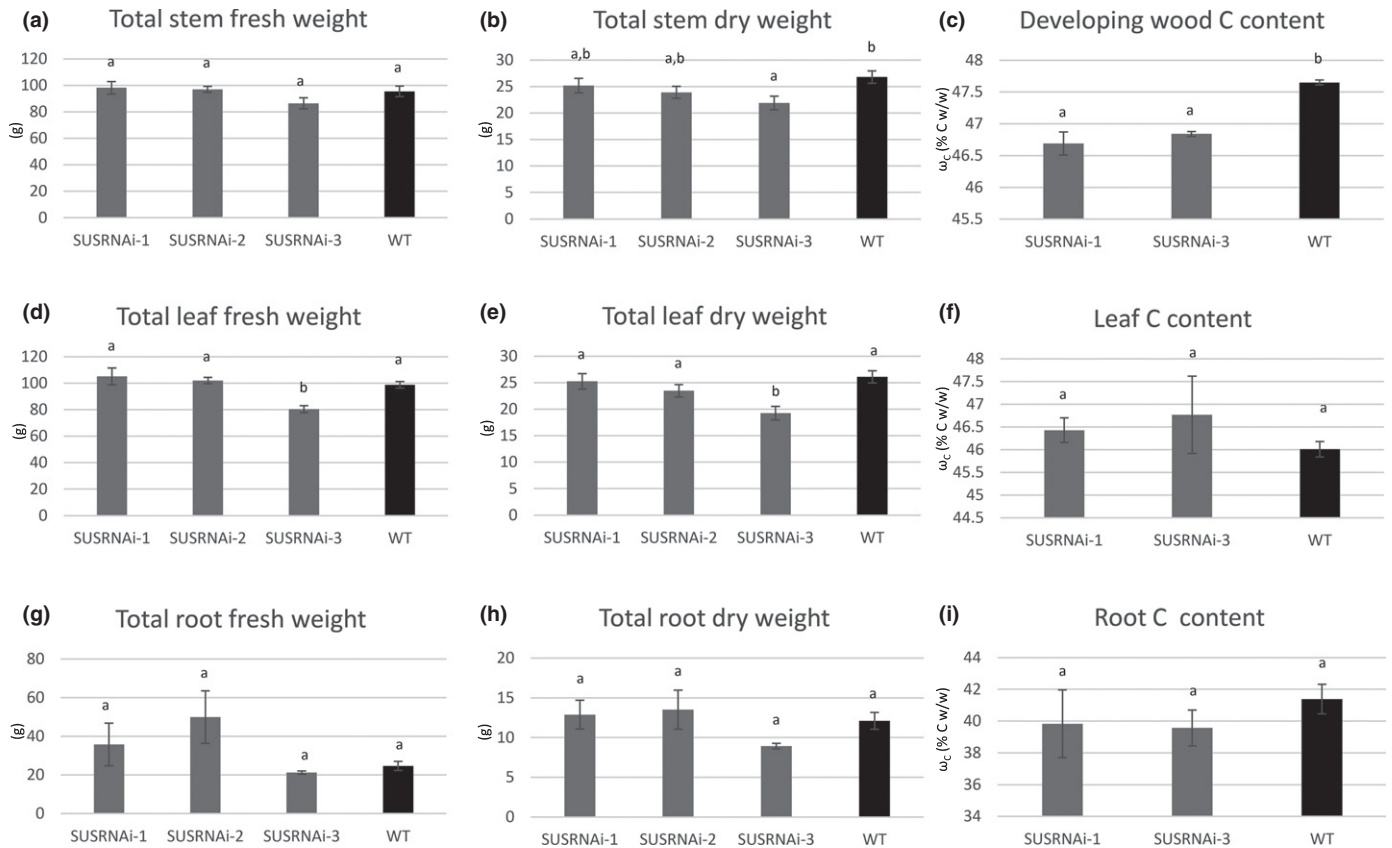
^{13}C tracking in *SUSRNAi* lines revealed altered sucrose turnover and C flow at the whole tree level

To investigate C fluxes between organs and at the whole tree level, we developed a $^{13}CO_2$ labelling system based on a previously reported design (Mahboubi *et al.*, 2013, 2015) and used it to characterize the C fluxes in *SUSRNAi-1* and *SUSRNAi-3* during a $^{13}CO_2$ pulse. Mahboubi *et al.* (2013) showed that ^{13}C can be detected in developing wood after a 4-h exposure to $^{13}CO_2$. We therefore exposed 6-wk-old *SUSRNAi* and WT trees to a $^{13}CO_2$ pulse and collected samples 4, 6, and 8 h after the pulse

start. The ^{13}C metabolic fate in leaves, roots, and developing wood was monitored using GC-MS. In parallel, we measured the total metabolite pools. While the total pool measurements provided a picture of the metabolic status of the tissues at fixed time points, the ^{13}C labelling experiments yielded insights into the movement of the ^{13}C among metabolites.

In leaves, during active photosynthesis sucrose is derived from the Calvin cycle (Fig. 3a). Sucrose showed decreased ^{13}C labelling at time 6 in both lines and at time 4 in *SUSRNAi-3*. Fructose and glucose did not show significant differences. The labelling of Krebs cycle metabolites was not altered, except for fumarate, which was increased at time 8. The ^{13}C-aspartate, ^{13}C-serine, ^{13}C-phenylalanine, and ^{13}C-glutamate were decreased in both lines at time 6. The ^{13}C-threonine was decreased at time 4 in both lines, while ^{13}C-glycerate was decreased in *SUSRNAi-1* at time 6. Total pools were unchanged, except for succinate and ketoglutarate in *SUSRNAi-1* (Table S5). Thus, the C flow changes in *SUSRNAi* leaves were primarily evident in the analysed amino acids.

The total sucrose levels in the phloem of the *SUSRNAi* lines were unchanged from those in the WT, but the ^{13}C

Fig. 2 Phenotype of 2-month-old wild-type (WT) and *SUSRNAi* hybrid aspen (*Populus tremula* × *tremuloides*) trees grown in the glasshouse. Top panels: total stem fresh weight (a), total stem dry weight (b), and C content of developing wood (c). Middle panels: total leaf fresh weight (d), dry weight (e), and C content (f). Bottom panels: root fresh weight (g), dry weight (h) and C content (i). Mass fraction of C was measured by IRMS. Bars indicate the average and error bars indicate the standard error. ANOVA, Duncan test, $n = 4$. Different letters indicate significant differences ($P < 0.05$).
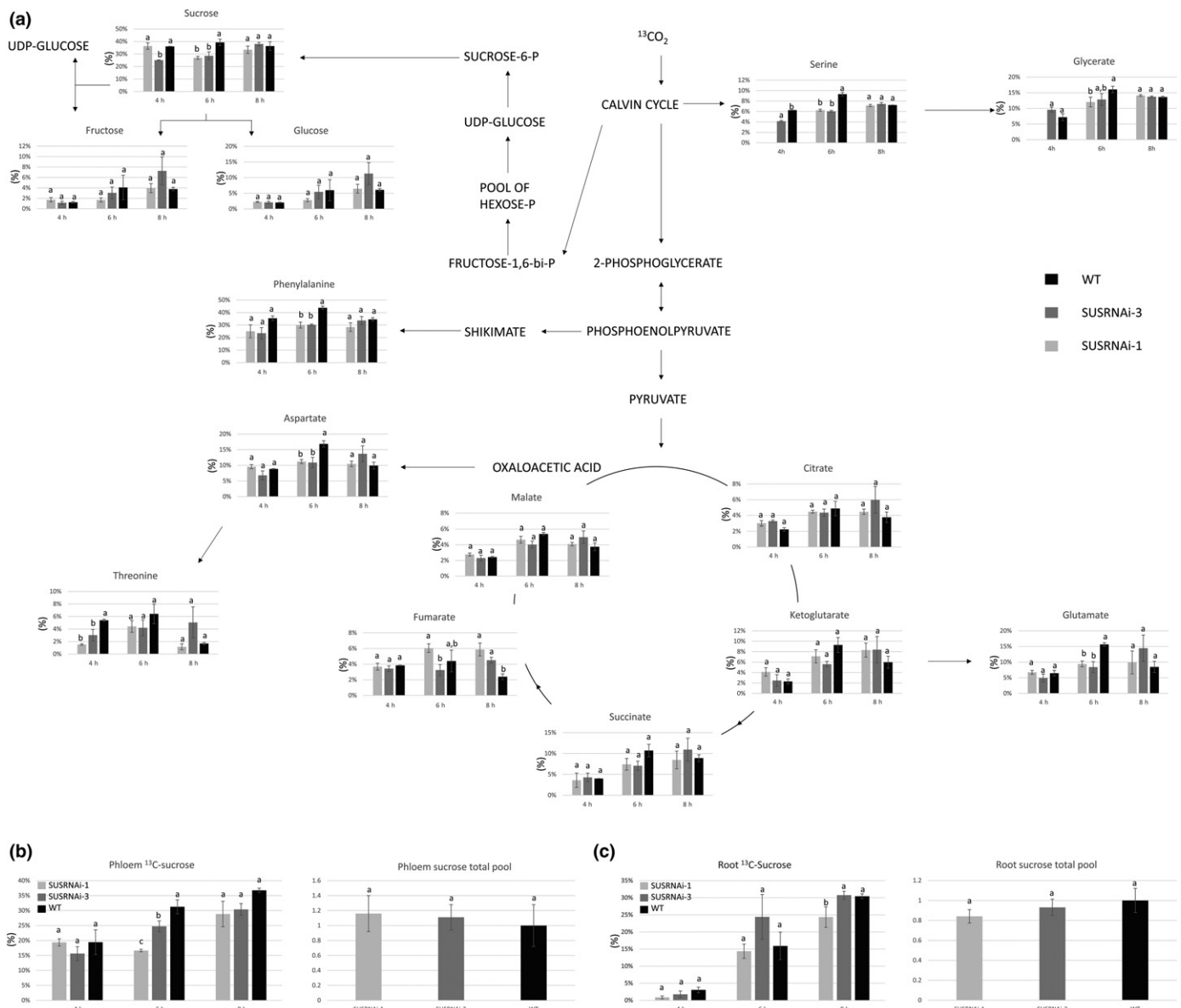
incorporation rate into the phloem sucrose pool was reduced in both *SUSRNAi* lines at time 6 (Fig. 3b), suggesting that *SUSRNAi* reduced the phloem sucrose loading rates.

Carbon in roots is derived from sucrose imported via the phloem. Root ¹³C-sucrose was only reduced in *SUSRNAi-1* at time 8 (Fig. 3c), while ¹³C-fructose and ¹³C-glucose did not show changes (Supporting Information Fig. S1). The same was observed for the Krebs cycle metabolites ¹³C-citrate, ¹³C-malate and ¹³C-succinate. However, ¹³C-ketoglutarate level was reduced in both lines at time 4 and time 6, and in *SUSRNAi-1* at time 8. The ¹³C-glutamate, ¹³C-aspartate, ¹³C-phenylalanine and ¹³C-serine did not show differences, but both lines showed decreased levels of ¹³C-valine at time 8 and of ¹³C-shikimate at time 6. Total pools for these metabolites did not differ significantly from WT (Fig. 3c; Table S6). Therefore, *SUSRNAi* changed the ¹³C flow through some individual metabolite pools in the roots, but there was no overall change.

Sucrose import fuels the central metabolism also in developing wood (Fig. 4a). The ¹³C-sucrose enrichment in developing wood of *SUSRNAi* lines was decreased in comparison to WT in both lines at time 6 and in *SUSRNAi-1* at time 8. The ¹³C-glucose and ¹³C-fructose, which can be produced from sucrose cleavage, were reduced in *SUSRNAi-1* at time 8 and in both lines at time 6 and 8, respectively. Apart from ¹³C-malate, the Krebs cycle

metabolites showed alterations as well: ¹³C-citrate was reduced in *SUSRNAi-1* at time 6; ¹³C-ketoglutarate was reduced in both lines at time 6 and 8; ¹³C-succinate was reduced in *SUSRNAi-3* at times 4, 6 and 8; and ¹³C-fumarate was reduced in both lines at time 8. The amino acids ¹³C-serine and ¹³C-phenylalanine showed decreased enrichment in both lines at times 6 and 8. The ¹³C-glycine and ¹³C-glycerate, which derive from ¹³C-serine, were reduced in both lines at time 6 and reduced in *SUSRNAi-3* at time 8, respectively. The ¹³C-aspartate was reduced in *SUSRNAi-1* at time 6 and 8. The ¹³C-beta-alanine was reduced in *SUSRNAi-3* at time 4, while ¹³C-asparagine was reduced in *SUSRNAi-3* at time 4 and in both lines at time 6. The ¹³C-glutamate was reduced in *SUSRNAi-1* at time 6. The ¹³C-GABA and ¹³C-isoleucine did not show differences. Thus, there is an overall ¹³C distribution decrease in the central metabolites of developing wood in the transgenic trees, which is linked to the reduction in ¹³C-sucrose. Moreover, a PCA of these data clearly showed that the overall ¹³C labelling profile of the metabolism in transgenic lines differs from the WT trees (Fig. 4b).

Total sucrose levels in the *SUSRNAi* developing wood did not differ significantly from those in WT trees between 6 and 14 h after the start of the light period (Fig. S2). Total pools of glucose and fructose in developing wood were also not significantly changed. However, all the three sugar levels exhibited increasing
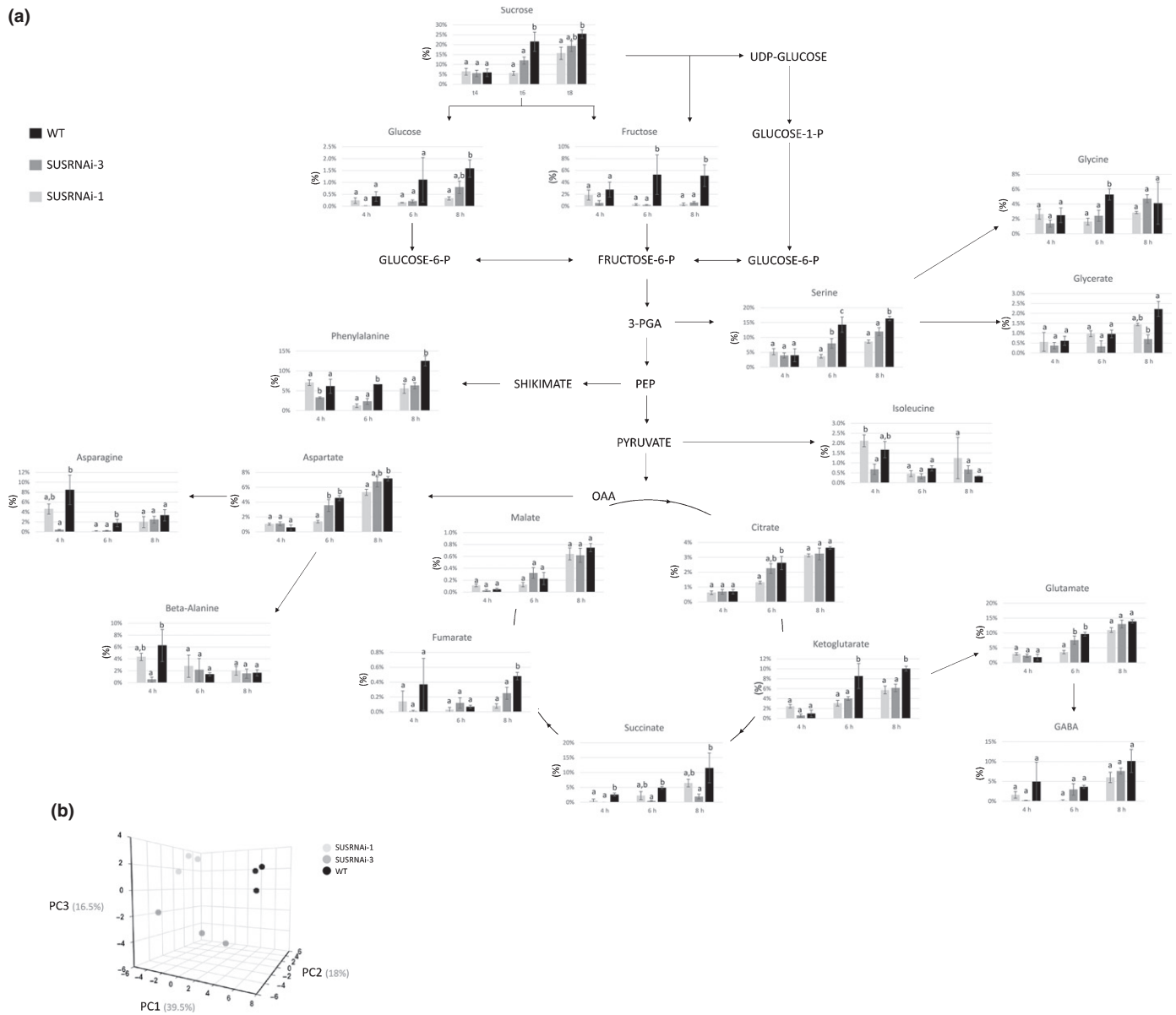
Fig. 3 Central metabolism in leaves (a) and sucrose metabolism in phloem (b) and roots (c) of 6-wk-old wild-type (WT) and *SUSRNAi* hybrid aspen (*Populus tremula × tremuloides*) trees grown in the glasshouse. Carbon-13 (^{13}C) enrichment of metabolites ((a) and left panels in (b) and (c)) and sucrose total pools (right panels in (b) and (c)) were measured by GC-MS. To obtain the ^{13}C enrichment of metabolites, trees were supplied with $^{13}CO_2$ for 4, 6 and 8 h. Total pool values in phloem and roots are relative to WT samples collected 6 h after the start of the light period. Bars indicate the average and error bars indicate the standard error. ANOVA, Duncan test, $n = 4$–3. Different letters indicate significant differences ($P < 0.05$).

trends at some time points. This is consistent with the results of Gerber *et al.* (2014), who observed a similar effect in the total pools of these sugars. The differences in significance between these two works may be due to the use of different analytical techniques and statistical methods. Most of the 14 other measured metabolites including aspartate, glycine and phenylalanine did not show differences between the *SUSRNAi* lines and the WT trees (Fig. S2). However, at one time point *SUSRNAi-3* contained increased levels of asparagine (8 h), glutamate (10 h) and serine (10 h), while for *SUSRNAi-1* increases were observed in beta-alanine (14 h) and isoleucine (10 h). The latter line also showed decreased levels in citrate (8 h), fumarate (6 h) and

malate (6 h). Both lines showed decreased levels in ketoglutarate (6 h). Succinate and glycerate had decreased levels in *SUSRNAi-1* (6 h) and increased levels in *SUSRNAi-3* (10 h). These findings show that the transgenic trees had alterations in the steady-state levels of some metabolites in developing wood, which are indicative of rearranged central metabolism in response to the reduced SUS activity.

The decreased ^{13}C-sucrose and the overall decreased ^{13}C labelling of central metabolites in developing wood strongly suggest that the total C decrease in this tissue in the transgenic lines (Fig. 2c) is due to the decreased sucrose incorporation. The decreased C flow in wood would have an impact on the

(a)

(b)

Fig. 4 Carbon-13 (^{13}C) labelling of metabolites of developing wood of 6-wk-old wild-type (WT) and *SUSRNAi* hybrid aspen (*Populus tremula* × *tremuloides*) trees grown in the glasshouse. Trees were supplied with $^{13}CO_2$ for 4, 6 and 8 h. (a) ^{13}C enrichment of central metabolites of developing wood measured by GC-MS. Columns indicate the average and error bars indicate the standard error. ANOVA, Duncan test, $n = 4$–3. Different letters indicate significant differences ($P < 0.05$). (b) Principal component analysis of the ^{13}C-metabolites shown in (a). The axes represent the first three principal components (PCs). The values between brackets indicate the variance of each PC. The data were standardized.

cell wall polymer biosynthesis. Indeed, the amounts of cellulose, lignin and hemicellulose per volume of wood were reduced in all the transgenic lines in comparison to WT (Gerber *et al.*, 2014). Thus, the alterations in the content of the polymers on a volume basis were due to an overall decrease in the C amount allocated to the cell walls. This conclusion was supported by NMR spectroscopy measurements comparing the ^{13}C content of *SUSRNAi-1* and WT cell wall polymers at times 0 and 8. The data point to a reduction in the ^{13}C levels in total cell wall (Fig. S3a), total G and S lignin (Fig. S3b) as well as in methoxy groups (Fig. S3c) and in individual structures related to lignin (Fig. S3d–g). With respect to cell wall carbohydrates, the effect

was more subtle although some individual peaks seem to have reduced labelling (Fig. S3b,h).

SUSRNAi does not affect starch levels in glasshouse grown trees

Starch is an important C sink and storage reserve in some tree tissues (Dietze *et al.*, 2014). Therefore, we measured starch levels in developing wood, mature wood, phloem, and source leaves to assess the possible role of SUS in starch metabolism in glasshouse grown aspen. No statistically significant differences between the transgenic and WT trees were found in any of the tissues

(Fig. S4). Worth noting is that the developing wood starch content of WT trees was 0.7 nmol of glucose per milligram fresh weight, which is equivalent to 0.013% (w/w) of fresh developing wood. Unda *et al.* (2017) found that in 5-month-old glasshouse-grown hybrid poplar starch accounted for *c.* 2.5% of developing wood on a dry weight basis. These amounts are well below the cell wall polymer contribution to developing wood biomass, which is above 80% (w/w) (Gandla *et al.*, 2015; Wang *et al.*, 2018). Thus, we found no evidence of SUS involvement in starch metabolism during active growth, or that starch would constitute a significant C sink in aspen developing wood.

SUSRNAi causes strong growth reduction under field conditions

Aspen trees in natural stands undergo seasonal growth and are exposed to many environmental stresses. Therefore, to fully evaluate the *SUSRNAi* effects on tree growth, we grew the transgenic trees in a 5-yr field experiment. The stem height and diameter of the *SUSRNAi* aspen trees were initially identical to those of WT trees but began to show growth defects in subsequent years. We observed consistent reduced height from year 4 onwards, while stem diameter was reduced at year 5 (Fig. 5a,b). The growth defects were more pronounced in *SUSRNAi-3*. In the fifth year the trees were cut, and the total aboveground biomass measured. The fresh and dry stem weights of the transgenic lines were reduced by up to 80% compared to those for WT trees (Fig. 5c, d). To confirm that the *SUSRNAi* was still functional in the transgenics, *SUS2* expression was assessed by qPCR and shown to be reduced (Fig. S5). These data prove that SUS is critical for aspen growth and biomass accumulation under field conditions.

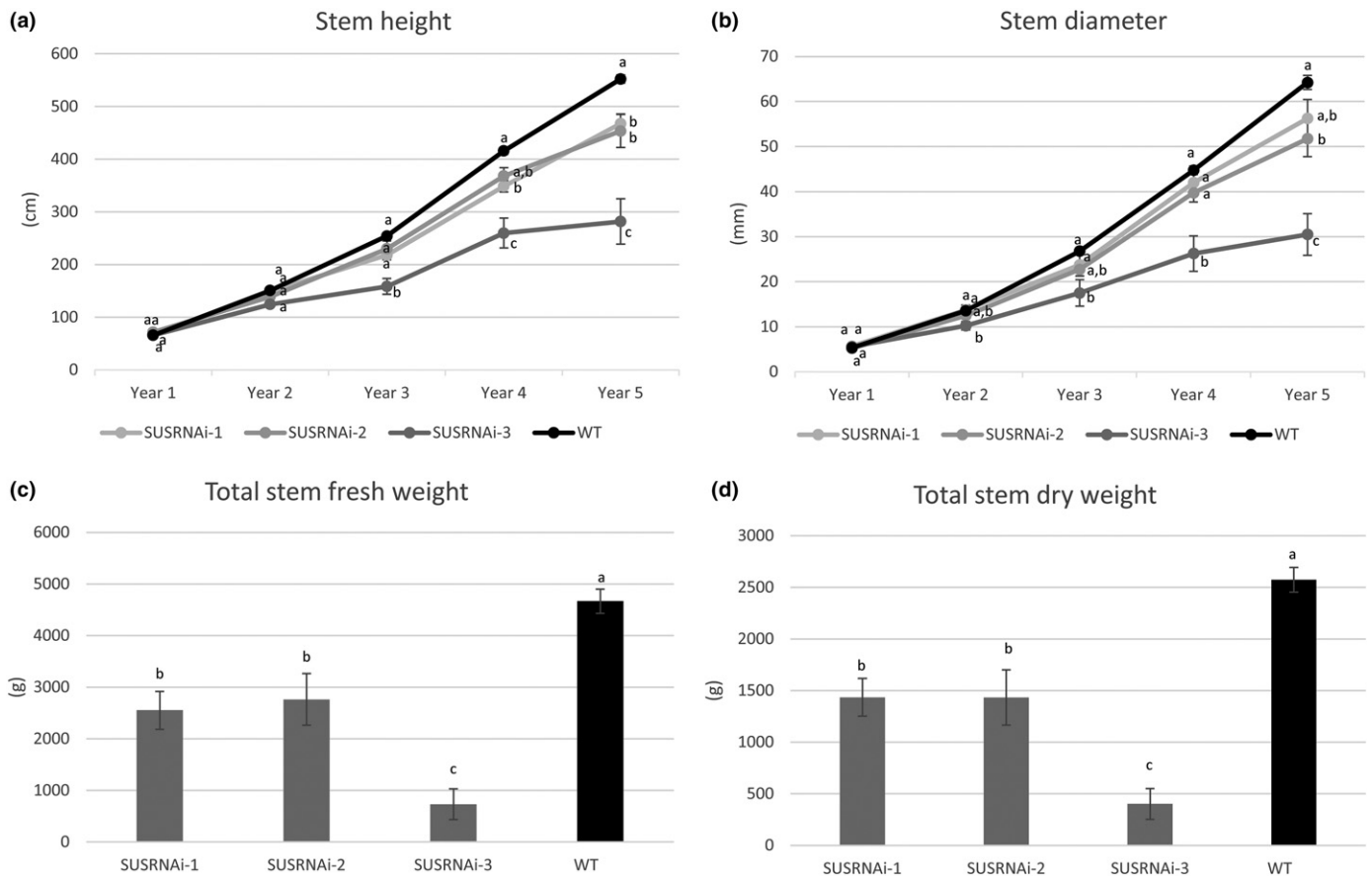### Acid invertase activity is increased in glasshouse *SUSRNAi* lines

Despite the metabolic changes in the *SUSRNAi* lines, stem biomass was only slightly reduced in the glasshouse-grown transgenic lines (Fig. 2). Since sucrose in the sink tissues is cleaved either by SUS or invertases, we hypothesized that invertases may compensate for SUS defects in the transgenics. Interestingly, the cytosolic neutral invertase activity in the developing wood of *SUSRNAi* lines was comparable to that of WT trees, but the acid invertase activity was increased (Fig. 6). This suggests that the acid invertase activity located in the apoplast and/or vacuoles can compensate for the lost SUS activity. However, the observed reduction in total C (Fig. 2c), and ^{13}C labelling over time (Fig. 4) in the developing wood of glasshouse-grown trees suggest that the acid invertase compensation was only partial. Moreover, field grown lines began to show a consistent reduction in stem height from year 4 and in stem diameter at year 5 (Fig. 5), suggesting that a partial compensation mechanism also operates under field conditions. Thus, the sustained reduction in SUS activity over multiple years under field conditions led to accumulative impairment of C incorporation to wood causing biomass reduction. Therefore, it can be concluded that SUS activity is a central determinant of wood formation and tree growth.
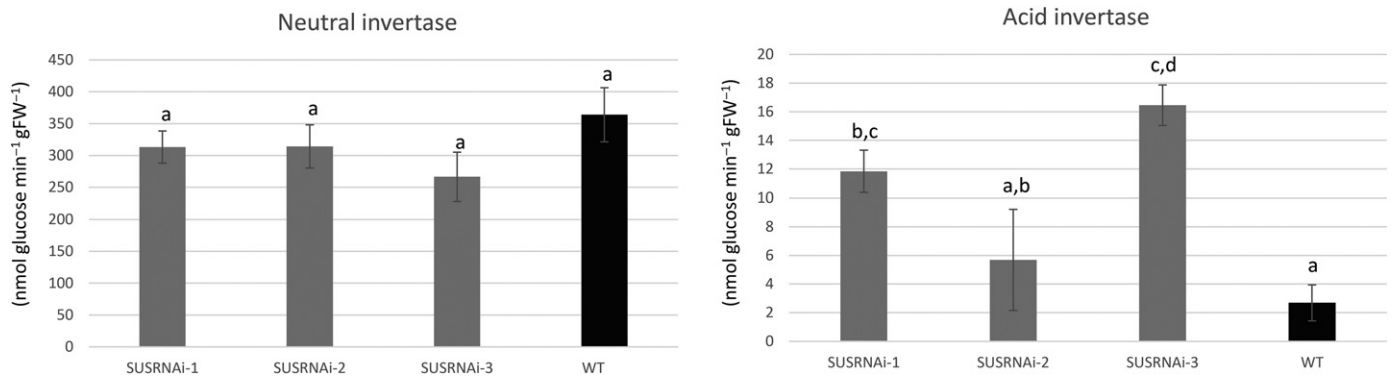
Discussion

Our results show that field grown *SUSRNAi* trees accumulate less stem biomass (Fig. 5), and the glasshouse grown transgenics contain less total C in developing wood (Fig. 2). Since stem biomass formation is dependent on the C derived from sucrose metabolism in sink tissues (Lemoine *et al.*, 2013; Ruan, 2014), we performed labelling experiments with $^{13}CO_2$ to investigate whether the reduced biomass and total C could be ascribed to altered ^{13}C-sucrose transport and/or metabolism in the transgenic lines. The reduced ^{13}C-sucrose in the developing wood of *SUSRNAi* trees suggested a reduction in sucrose import (Fig. 4a). The reduced ^{13}C-sucrose level in developing wood (Fig. 4) is also consistent with a reduction in *de novo* sucrose synthesis, however this process is not believed to contribute significantly to the C flux during wood formation (Roach *et al.*, 2017). The reduction in ^{13}C sucrose was reflected in the decreased ^{13}C labelling of many central metabolites (Fig. 4a); this trend was also observed for the ^{13}C accumulation in cell wall polymers (Fig. S3). Since also the cell wall polymer mass per volume unit is reduced in the transgenic lines (Gerber *et al.*, 2014), it can be concluded that C allocation to cell walls is decreased and the cause of the biomass loss (Fig. 5).

The mild phenotype of the glasshouse grown *SUSRNAi* trees (Fig. 2b) suggested the existence of an alternative compensatory sucrose cleavage mechanism involving invertases. We observed no significant changes in neutral invertase activity in the *SUSRNAi* lines, but the acid invertase activity was increased (Fig. 6). Compensation by acid invertases when SUS activity is reduced has also been reported in other species (Zrenner *et al.*, 1995; Baroja-Fernández *et al.*, 2009). The increased acid invertase activity also suggests that these invertases influence C allocation in developing wood. Cell wall acid invertases have coevolved with the vasculature and are believed to contribute to phloem unloading (Wan *et al.*, 2018). The tendency of increased glucose and fructose levels (Fig. S2) in *SUSRNAi* trees resembles that seen in potato tubers with reduced SUS, in which the hexose increase was attributed to a compensatory increase in invertase (Zrenner *et al.*, 1995). A similar compensation mechanism may also function in the developing wood of *SUSRNAi* trees. However, the observed phenotypes in the transgenics including the reduction in total C (Fig. 2c) and ^{13}C-metabolite labelling (Fig. 4) suggest that acid invertases only partially compensate for the SUS loss. This explanation is in line with the gradual growth reduction in the field grown *SUSRNAi* trees (Fig. 5). The seasonal changes and environmental effects under natural field conditions are likely to exacerbate this effect. Environmental stress conditions have been shown to exacerbate SUS defect phenotypes in other species (Ricard *et al.*, 1998; Wang *et al.*, 2014; Takehara *et al.*, 2018). Moreover, in aspen seasonal changes in SUS activity were observed in the outer trunk wood (Schrader & Sauter, 2002), suggesting that SUS may be involved in the activity–dormancy and dormancy–activity transitions.

SUS catalyses the sucrose degradation into fructose and UDP-glucose, the latter being the substrate for cellulose synthesis. Although it has often been hypothesized that SUS is essential for directly providing UDP-glucose to the cellulose synthase complex

(a) Stem height

(b) Stem diameter

(c) Total stem fresh weight

(d) Total stem dry weight

Fig. 5 Phenotype of wild-type (WT) and *SUSRNAi* hybrid aspen (*Populus tremula × tremuloides*) trees grown during 5 yr in the field. (a) Stem height and (b) stem diameter over time. (c) Total stem fresh weight, and (d) dry weight at harvest in the fifth year. Data points and bars indicate the average and error bars indicate the standard error. ANOVA, Duncan test, $n = 4$. Different letters indicate significant differences ($P < 0.05$).

Neutral invertase

Acid invertase

Fig. 6 Neutral and acid invertase activity in developing wood of 6-wk-old wild-type (WT) and *SUSRNAi* hybrid aspen (*Populus tremula × tremuloides*) trees grown in the glasshouse. Bars indicate the average and error bars indicate the standard error. ANOVA, Duncan test, $n = 5$–4. Different letters indicate significant differences ($P < 0.05$).

(Amor *et al.*, 1995; Haigler *et al.*, 2001; Stein & Granot, 2019), near complete silencing of SUS in aspen developing wood did not abolish cellulose biosynthesis (Gerber *et al.*, 2014). However, SUS overexpression in aspen can increase the cellulose content (Coleman *et al.*, 2009). Consequently, SUS can contribute to the UDP-glucose provision for cellulose synthesis in aspen trees but is not essential for this process. Instead, cytosolic invertase

silencing significantly reduced cellulose levels in developing wood of aspen, suggesting that the cellulose biosynthesis pathway involves hexokinase and UDP-glucose pyrophosphorylase (Rende *et al.*, 2017), while SUS plays an essential role in controlling total C allocation.

When leaves transition from sink to source tissues, SUS levels fall significantly (Nguyen-Quoc *et al.*, 1990; Qiu *et al.*, 2007;

Zhu *et al.*, 2018). Consequently, SUS levels in mature leaves are low (Pavlinova *et al.*, 2002; Thirugnanasambandam *et al.*, 2019). In line with this, SUS activity in source leaves of glasshouse grown aspens was close to the background level. Leaf SUS is thought to be involved in sucrose degradation during the day (Rolland *et al.*, 2006). Hence, several mechanisms could be affecting the sucrose labelling in the SUS leaves (Fig. 3a), including reduced sucrose synthesis, or differential labelling kinetics of the different subcellular sucrose pools (Kruger *et al.*, 2007; Fernie & Morgan, 2013; Beshir *et al.*, 2017). Moreover, the alteration in ^{13}C labelling is not limited to sucrose in leaves, but several other central metabolites also show differences, especially amino acids (Fig. 3a). This may be considered a regulatory effect generated locally in the leaves or triggered by a sink-to-source signal from the developing wood in response to the reduced sucrose and C allocation (Ainsworth & Bush, 2011). However, the *SUSRNAi* source leaves do not show marked phenotypic (Fig. 2; Tables S3, S4) or metabolite pool alterations (Fig. S4d; Table S5), which suggests that SUS does not have an essential role in these leaves during active growth.

The role of SUS in aspen roots under glasshouse conditions seems even more limited. The fact that the roots of *SUSRNAi* lines show no phenotypic alterations (Fig. 2g–i) and that they have a few metabolites with altered ^{13}C labelling (Fig. S1) suggests that they can compensate for the reduced SUS activity. Similarly, no obvious role for SUS was observed in maize roots under aerobic conditions, but it was important under anaerobic condition such as caused by flooding (Ricard *et al.*, 1998). However, it is also possible that the limited effect of SUS silencing in aspen roots was due to residual SUS activity in this tissue.

Because all the analysed tissues had reduced SUS activity or reduced *SUS* mRNA levels, it is probable that the observed effects are initiated locally. This is especially true for developing wood, which has high SUS activity in WT and only residual SUS activity in the *SUSRNAi* lines (Fig. 1). However, systemic effects could be occurring simultaneously, including additive effects on the ^{13}C-sucrose transport across tissues. This is illustrated by the decreased ^{13}C-sucrose enrichment in the source to sink transport direction in the *SUSRNAi* lines (Figs 3, 4), especially from phloem towards developing wood. Since SUS has such low levels in source leaves (Fig. 1), it is not likely that the effect seen in developing wood is merely an effect generated in the leaves and then cascaded to the sink tissues. However, a feedback regulation produced by the reduced developing wood sink activity, which would impact the C metabolism in leaves, is possible (Ainsworth & Bush, 2011). Probing such a mechanism could be done through grafting experiments testing different combinations of WT and *SUSRNAi* scions and stocks. Indeed, the C flow alteration at the whole tree level together with the altered sucrose turnover in leaves, phloem and developing wood raises the interesting possibility that SUS could participate in a signal generation involved in the source–sink metabolic coordination.

To summarize, the decrease in SUS activity leads to decreased sucrose C incorporation in developing wood, which is subsequently reflected in the decreased C flow in the central metabolism. This determines a lower C allocation whose output is a reduced total C and reduced biomass in wood. This provides evidence that SUS is involved in determining C allocation in aspen developing wood and, thus, in affecting the biomass accumulation into this tissue. Likewise, SUS silencing affects the C metabolism at the whole tree level as shown through ^{13}C labelling. The alteration in C metabolism at the whole tree level suggests that SUS could participate in the sink–source metabolic coordination.

Author contributions

PGD planned and performed experiments and analysed data; TN planned experiments and analysed data; IT performed the chlorophyll fluorescence determinations and analysed data; AB performed experiments; MH performed the NMR measurements and analyses; ED, MD-M and EJM performed the field experiment and analysed field data; PGD and TN wrote the manuscript with contributions from all the authors. ED and MD-M contributed equally to this work.

ORCID

Pia Guadalupe Dominguez https://orcid.org/0000-0003-0413-2273
Evgeniy Donev https://orcid.org/0000-0002-7279-0481
Marta Derba-Maceluch https://orcid.org/0000-0002-8034-3630
Mattias Hedenström https://orcid.org/0000-0002-0903-6662
Ewa J. Mellerowicz https://orcid.org/0000-0001-6817-1031
Totte Niittylä https://orcid.org/0000-0001-8029-1503
Ivana Tomášková https://orcid.org/0000-0001-6219-5980

References

Ainsworth EA, Bush DR. 2011. Carbohydrate export from the leaf: a highly regulated process and target to enhance photosynthesis and productivity. *Plant Physiology* **155**: 64–69.

Amor Y, Haigler CH, Johnson S, Wainscott M, Delmer DP. 1995. A membrane-associated form of sucrose synthase and its potential role in synthesis of cellulose and callose in plants. *Proceedings of the National Academy of Sciences, USA* **92**: 9353–9357.

Baker NR. 2008. Chlorophyll fluorescence: a probe of photosynthesis *in vivo*. *Annual Review of Plant Biology* **59**: 89–113.

Baroja-Fernández E, Muñoz FJ, Montero M, Etxeberria E, Sesma MT, Ovecka M, Bahaji A, Ezquer I, Li J, Prat S *et al.* 2009. Enhancing sucrose synthase activity in transgenic potato (*Solanum tuberosum* L.) tubers results in increased levels of starch, ADPglucose and UDPglucose and total yield. *Plant & Cell Physiology* 50: 1651–1662.

Beshir WF, Mbong VBM, Hertog MLATM, Geeraerd AH, Van Den Ende W, Nicolaï BM. 2017. Dynamic labeling reveals temporal changes in carbon re-allocation within the central metabolism of developing apple fruit. *Frontiers in Plant Science* 8: 1–16.

Busov VB. 2018. Manipulation of growth and architectural characteristics in trees for increased woody biomass production. *Frontiers in Plant Science* 871: 1–8.

Chaffey N, Barlow P. 2001. The cytoskeleton facilitates a three-dimensional symplasmic continuum in the long-lived ray and axial parenchyma cells of angiosperm trees. *Planta* 213: 811–823.

Cheng WH, Taliercio EW, Chourey PS. 1996. The Miniature1 seed locus of maize encodes a cell wall invertase required for normal development of endosperm and maternal cells in the pedicel. *Plant Cell* 8: 971–983.

Coleman HD, Ellis DD, Gilbert M, Mansfield SD. 2006. Up-regulation of sucrose synthase and UDP-glucose pyrophosphorylase impacts plant growth and metabolism. *Plant Biotechnology Journal* 4: 87–101.

Coleman HD, Yan J, Mansfield SD. 2009. Sucrose synthase affects carbon partitioning to increase cellulose production and altered cell wall ultrastructure. *Proceedings of the National Academy of Sciences, USA* 106: 13118–13123.

D'Aoust MA, Yelle S, Nguyen-Quoc B. 1999. Antisense inhibition of tomato fruit sucrose synthase decreases fruit setting and the sucrose unloading capacity of young fruit. *Plant Cell* 11: 2407–2418.

Dietze MC, Sala A, Carbone MS, Czimczik CI, Mantooth JA, Richardson AD, Vargas R. 2014. Nonstructural carbon in woody plants. *Annual Review of Plant Biology* 65: 667–687.

Dubouzet JG, Strabala TJ, Wagner A. 2013. Potential transgenic routes to increase tree biomass. *Plant Science* 212: 72–101.

Fernie AR, Morgan JA. 2013. Analysis of metabolic flux using dynamic labelling and metabolic modelling. *Plant, Cell & Environment* 36: 1738–1750.

Gandla ML, Derba-Maceluch M, Liu X, Gerber L, Master ER, Mellerowicz EJ, Jönsson LJ. 2015. Expression of a fungal glucuronoyl esterase in populus: effects on wood properties and saccharification efficiency. *Phytochemistry* 112: 210–220.

Gerber L, Zhang B, Roach M, Rende U, Gorzsás A, Kumar M, Burgert I, Niittylä T, Sundberg B. 2014. Deficient sucrose synthase activity in developing wood does not specifically affect cellulose biosynthesis, but causes an overall decrease in cell wall polymers. *New Phytologist* 203: 1220–1230.

Gullberg J, Jonsson P, Nordström A, Sjöström M, Moritz T. 2004. Design of experiments: an efficient strategy to identify factors influencing extraction and derivatization of *Arabidopsis thaliana* samples in metabolomic studies with gas chromatography/mass spectrometry. *Analytical Biochemistry* 331: 283–295.

Haigler C, Ivanova-Datcheva M, Hogan P, Salnikov V, Hwang S, Martin K, Delmer D. 2001. Carbon partitioning to cellulose synthesis. *Plant Molecular Biology* 47: 29–51.

Hedenström M, Wiklund-Lindström S, Öman T, Lu F, Gerber L, Schatz P, Sundberg B, Ralph J. 2009. Identification of lignin and polysaccharide modifications in populus wood by chemometric analysis of 2D NMR spectra from dissolved cell walls. *Molecular Plant* 2: 933–942.

Hubbard NL, Huber SC, Pharr DM. 1989. Sucrose phosphate synthase and acid invertase as determinants of sucrose concentration in developing muskmelon (*Cucumis melo* L.) fruits. *Plant Physiology* 91: 1527–1534.

Kim H, Ralph J, Akiyama T. 2008. Solution-state 2D NMR of ball-milled plant cell wall gels in DMSO-d6. *BioEnergy Research* 1: 56–66.

Kruger N, Le Lay P, Ratcliffe R. 2007. Vacuolar compartmentation complicates the steady-state analysis of glucose metabolism and forces reappraisal of sucrose cycling in plants. *Phytochemistry* 68: 2189–2196.

Lemoine R, La Camera S, Atanassova R, Dédaldéchamp F, Allario T, Pourtau N, Bonnemain JL, Laloi M, Coutos-Thévenot P, Maurousset L *et al.* 2013. Source-to-sink transport of sugar and regulation by environmental factors. *Frontiers in Plant Science* 4: 1–21.

Li B, Liu H, Zhang Y, Kang T, Zhang L, Tong J, Xiao L, Zhang H. 2013. Constitutive expression of cell wall invertase genes increases grain yield and starch content in maize. *Plant Biotechnology Journal* 11: 1080–1091.

Lindén P, Keech O, Stenlund H, Gardeström P, Moritz T. 2016. Reduced mitochondrial malate dehydrogenase activity has a strong effect on photorespiratory metabolism as revealed by ^{13}C labelling. *Journal of Experimental Botany* 67: 3123–3135.

Mahboubi A, Linden P, Hedenström M, Moritz T, Niittylä T. 2015. ^{13}C tracking after $^{13}CO_2$ supply revealed diurnal patterns of wood formation in aspen. *Plant Physiology* 168: 478–489.

Mahboubi A, Niittylä T. 2018. Sucrose transport and carbon fluxes during wood formation. *Physiologia Plantarum* 164: 67–81.

Mahboubi A, Ratke C, Gorzsás A, Kumar M, Mellerowicz EJ, Niittylä T. 2013. Aspen SUCROSE TRANSPORTER3 allocates carbon into wood fibers. *Plant Physiology* 163: 1729–1740.

Maxwell K, Johnson G. 2000. Chlorophyll fluorescence – a practical guide. *Journal of Experimental Botany* 51: 659–668.

Morey SR, Hirose T, Hashida Y, Miyao A, Hirochika H, Ohsugi R, Yamagishi J, Aoki N. 2018. Genetic evidence for the role of a rice vacuolar invertase as a molecular sink strength determinant. *Rice* 11: 6.

Nguyen-Quoc B, Krivitzky M, Huber SC, Lecharny A. 1990. Sucrose synthase in developing maize leaves: regulation of activity by protein level during the import to export transition. *Plant Physiology* 94: 516–523.

Novaes E, Osorio L, Drost DR, Miles BL, Boaventura-Novaes CRD, Benedict C, Dervinis C, Yu Q, Sykes R, Davis M *et al.* 2009. Quantitative genetic analysis of biomass and wood chemistry of *Populus* under different nitrogen levels. *New Phytologist* 182: 878–890.

Pavlinova OA, Balakhontsev EN, Prasolova MF, Turkina MV. 2002. Sucrose-phosphate synthase, sucrose synthase, and invertase in sugar beet leaves. *Russian Journal of Plant Physiology* 49: 68–73.

Pfaffl MW. 2001. A new mathematical model for relative quantification in real-time RT-PCR. *Nucleic Acids Research* 29: 45e–45.

Plomion C, Leprovost G, Stokes A. 2001. Wood formation in trees. *Plant Physiology* 127: 1513–1523.

Qiu QS, Hardin SC, Mace J, Brutnell TP, Huber SC. 2007. Light and metabolic signals control the selective degradation of sucrose synthase in maize leaves during deetiolation. *Plant Physiology* 144: 468–478.

Rende, U, Wang, W, Gandla, ML, Jönsson, LJ & Niittylä, T. 2016. Cytosolic invertase contributes to the supply of substrate for cellulose biosynthesis in developing wood. *New Phytologist* 214: 796–807.

Rende U, Wang W, Gandla ML, Jönsson LJ, Niittylä T. 2017. Cytosolic invertase contributes to the supply of substrate for cellulose biosynthesis in developing wood. *New Phytologist* 214: 796–807.

Rennie EA, Turgeon R. 2009. A comprehensive picture of phloem loading strategies. *Proceedings of the National Academy of Sciences, USA* 106: 14162–14167.

Ricard B, VanToai T, Chourey P, Saglio P. 1998. Evidence for the critical role of sucrose synthase for anoxic tolerance of maize roots using a double mutant. *Plant Physiology* 116: 1323–1331.

Roach M, Arrivault S, Mahboubi A, Krohn N, Sulpice R, Stitt M, Niittylä T. 2017. Spatially resolved metabolic analysis reveals a central role for transcriptional control in carbon allocation to wood. *Journal of Experimental Botany* 68: 3529–3539.

Rolland F, Baena-Gonzalez E, Sheen J. 2006. Sugar sensing and signaling in plants: conserved and novel mechanisms. *Annual Review of Plant Biology* 57: 675–709.

Ruan Y-L. 2014. Sucrose metabolism: gateway to diverse carbon use and sugar signaling. *Annual Review of Plant Biology* 65: 33–67.

Schrader S, Sauter JJ. 2002. Seasonal changes of sucrose-phosphate synthase and sucrose synthase activities in poplar wood (*Populus x canadensis* Moench 'robusta') and their possible role in carbohydrate metabolism. *Journal of Plant Physiology* 159: 833–843.

Sheen J. 1990. Metabolic repression of transcription in higher plants. *Plant Cell* 2: 1027–1038.

Smith AM, Zeeman SC. 2006. Quantification of starch in plant tissues. *Nature Protocols* 1: 1342–1345.

Sonnewald U, Fernie AR. 2018. Next-generation strategies for understanding and influencing source–sink relations in crop plants. *Current Opinion in Plant Biology* 43: 63–70.

Stein O, Granot D. 2019. An overview of sucrose synthases in plants. *Frontiers in Plant Science* 10: 1–14.

Stirbet A, Govindjee. 2011. On the relation between the Kautsky effect (chlorophyll a fluorescence induction) and Photosystem II: basics and applications of the OJIP fluorescence transient. *Journal of Photochemistry and Photobiology B: Biology* 104: 236–257.

Szecowka M, Heise R, Tohge T, Nunes-Nesi A, Vosloh D, Huege J, Feil R, Lunn J, Nikoloski Z, Stitt M et al. 2013. Metabolic fluxes in an illuminated Arabidopsis rosette. *Plant Cell* 25: 694–714.

Takehara K, Murata K, Yamaguchi T, Yamaguchi K, Chaya G, Kido S, Iwasaki Y, Ogiwara H, Ebitani T, Miura K. 2018. Thermo-responsive allele of sucrose synthase 3 (Sus3) provides high-temperature tolerance during the ripening stage in rice (*Oryza sativa* L.). *Breeding Science* 68: 336–342.

Thirugnanasambandam PP, Mason PJ, Hoang NV, Furtado A, Botha FC, Henry RJ. 2019. Analysis of the diversity and tissue specificity of sucrose synthase genes in the long read transcriptome of sugarcane. *BMC Plant Biology* 19: 1–14.

Unda F, Kim H, Hefer C, Ralph J, Mansfield SD. 2017. Altering carbon allocation in hybrid poplar (*Populus alba × grandidentata*) impacts cell wall growth and development. *Plant Biotechnology Journal* 15: 865–878.

Untergasser A, Cutcutache I, Koressaar T, Ye J, Faircloth BC, Remm M, Rozen SG. 2012. Primer3 – new capabilities and interfaces. *Nucleic Acids Research* 40: 1–12.

Van Bel AJE. 1990. Xylem-phloem exchange via the rays: the undervalued route of transport. *Journal of Experimental Botany* 41: 631–644.

Wan H, Wu L, Yang Y, Zhou G, Ruan YL. 2018. Evolution of sucrose metabolism: the dichotomy of invertases and beyond. *Trends in Plant Science* 23: 163–177.

Wang H, Sui X, Guo J, Wang Z, Cheng J, Ma S, Li X, Zhang Z. 2014. Antisense suppression of cucumber (*Cucumis sativus* L.) sucrose synthase 3 (CsSUS3) reduces hypoxic stress tolerance. *Plant, Cell & Environment* 37: 795–810.

Wang Z, Winestrand S, Gillgren T, Jönsson LJ. 2018. Chemical and structural factors influencing enzymatic saccharification of wood from aspen, birch and spruce. *Biomass and Bioenergy* 109: 125–134.

Wei Z, Qu Z, Zhang L, Zhao S, Bi Z, Ji X, Wang X, Wei H. 2015. Overexpression of poplar xylem sucrose synthase in tobacco leads to a thickened cell wall and increased height. *PLoS ONE* 10: 1–20.

Yu SM, Lo SF, Ho THD. 2015. Source-sink communication: regulated by hormone, nutrient, and stress cross-signaling. *Trends in Plant Science* 20: 844–857.

Zhang C, Han L, Slewinski TL, Sun J, Zhang J, Wang ZY, Turgeon R. 2014. Symplastic phloem loading in poplar. *Plant Physiology* 166: 306–313.

Zhang D, Xu B, Yang X, Zhang Z, Li B. 2011. The sucrose synthase gene family in *Populus*: structure, expression, and evolution. *Tree Genetics and Genomes* 7: 443–456.

Zhu J, Qi J, Fang Y, Xiao X, Li J, Lan J, Tang C. 2018. Characterization of sugar contents and sucrose metabolizing enzymes in developing leaves of *Hevea brasiliensis*. *Frontiers in Plant Science* 9: 1–11.

Zrenner R, Salanoubat M, Willmitzer L, Sonnewald U. 1995. Evidence of the crucial role of sucrose synthase for sink strength using transgenic potato plants (*Solanum tuberosum* L.). *The Plant Journal* 7: 97–107.

Supporting Information

Additional Supporting Information may be found online in the Supporting Information section at the end of the article.

Fig. S1 ^{13}C labelling of central metabolites of roots of 6-wk-old SUS trees.

Fig. S2 Metabolite total pool content measured in developing wood by GC-MS.

Fig. S3 ^{13}C labelling of cell wall monomers of developing wood of 6-wk-old SUS trees measured by 2D-NMR.

Fig. S4 Starch content in developing wood, mature wood, phloem and leaves of SUS trees measured by the enzymatic method.

Fig. S5 *SUS2* mRNA levels in developing wood of SUS trees grown in the field measured by RT-qPCR.

Table S1 Primer list used in the qPCRs.

Table S2 Nitrogen balance index (NBI), chlorophyll index (CHL), flavonol index (FLV) and anthocyanin index (ANTH).

Table S3 Polyphasic chlorophyll fluorescence induction curve (OJIP transient).

Table S4 Light curve parameters measured with a portable fluorometer FluorPen FP100max.

Table S5 Total metabolite pools in leaves of 6-wk-old trees measured by GC-MS.

Table S6 Total metabolite pools in roots of 6-wk-old trees measured by GC-MS.

Please note: Wiley-Blackwell are not responsible for the content or functionality of any supporting information supplied by the authors. Any queries (other than missing material) should be directed to the *New Phytologist* Central Office.